Applied Catalysis B: Environmental 312 (2022) 121422

Contents lists available at ScienceDirect

Applied Catalysis B: Environmental

journal homepage: www.elsevier.com/locate/apcatb

Triboelectric pulsed direct-current enhanced radical generation for efficient degradation of organic pollutants in wastewater

Xinliang Liu [a], Jilong Mo [a], Wanhai Wu [a,b], Hainong Song [b], Shuangxi Nie [a,b,*]

[a] School of Light Industry and Food Engineering, Guangxi Key Laboratory of Clean Pulp & Papermaking and Pollution Control, Guangxi University, Nanning 530004
[b] Guangxi Bossco Environment Protecting Technology Co., Ltd, Nanning 530007, PR China

ARTICLE INFO

Keywords:
Triboelectric nanogenerator
Radical generation
Pulsed direct-current
4-chlorophenol
Waste water treatment

ABSTRACT

The generation of free radicals was enhanced by triboelectric pulsed direct-current during the organic pollutant degradation. The self-powered electrochemical system was constructed for enhancing 4-CP removal powered by a water-driven triboelectric nanogenerator (WD-TENG). The output of current, voltage, and power of WD-TENG were studied. The removal of 4-CP and its degradation mechanism were also discussed. The results shows that the formation of hydroxyl radicals (·OH) was improved by improving PMA(Mo^{5+}) conversion efficiency by the WD-TENG in the phosphomolybdic acid/H_2O_2 (PMA/H_2O_2) system, resulting the mineralizing the 4-CP via dichlorination and oxidation. The removal of 4-CP improved by 10% in 120 min in the WD-TENG powered electro-PMA/H_2O_2 system. This study provides a promising methodology for improving the performance of self-powered electrochemical processes for the treatment of environmental pollution.

1. Introduction

Pulping wastewater, one of the serious pollution sources, is hard to be treated [1]. Because bleaching process could lignin could be converted partly into absorbable organic halogen (AOX), kinds of persistent organic pollutants (POPs) by chlorine bleaching agents in pulping process [2,3], which can enrich in living organisms and produce lasting contamination. So advanced treatment technologies of pulping wastewater with high efficiency and low-carbon economy become a new topic and the inevitable way for green and sustainable development of pulping industry [4].

4-chlorophenol (4-CP), a kind of POPs, is used as the target compound in bleaching process [5]. 4-CP is highly toxic, colorless, and soluble in water. Its high solubility makes it one of the most highly dispersed toxic environmental pollutants. Thus, this pollutant must be maintained at very low concentrations in natural waters. Numerous technologies have been tested for chlorophenol removal, including electrochemical degradation [6,7], Fenton oxidation [8], sonochemical method [9], adsorption [10], photodegradation [11], catalytic hydrodechlorination [12], and biological processes [13]. However, several of these technologies has disadvantages, such as photo-oxidation requires expensive reagents; bioremediation requires applications at a high concentration; and physisorption might cause secondary pollution [12]. Among these, Fenton oxidation is a potentially advanced technology for wastewater treatment because it can generate hydroxyl radicals (·OH) [14].

The hydroxyl radical, a powerful oxidizing agent with a potential of 2.87 V vs standard hydrogen electrode (SHE), can mineralize pollutants into CO_2 and H_2O [15]. It can be produced by activating hydrogen peroxide using Fe, Cr, Cu, Mn, or phosphomolybdic acid [16–18]. However,·OH is unstable, can be quenched or caught by H_2O_2, and then chemically decomposes to oxygen [19,20]. Thus, these·OH radicals cannot be used effectively. Electrolysis can enhance electron transformation, which is considered to be the limit of the catalytic ability in this process [19,21]. It can also convert dissolved oxygen into hydrogen peroxide via two-electron oxygen reduction [22]. The predominant technology used is the electro-Fenton process. In the electro-Fenton process, the efficiency depends on the supporting electrolyte type, electrode material, concentration of pollutants, and electric current density [23]. However, its use is limited owing to the large amount of power consumption derived from fossil fuel combustion, low catalytic activity of the cathode catalyst for the formation of H_2O_2, and production of secondary pollutants in iron sludge [24,25]. Thus, electrolysis using non-fossil energy and high activity catalysts without iron is

* Corresponding author at: School of Light Industry and Food Engineering, Guangxi Key Laboratory of Clean Pulp & Papermaking and Pollution Control, Guangxi University, Nanning 530004.
E-mail address: nieshuangxi@gxu.edu.cn (S. Nie).

https://doi.org/10.1016/j.apcatb.2022.121422
Received 15 February 2022; Received in revised form 9 April 2022; Accepted 14 April 2022
Available online 19 April 2022

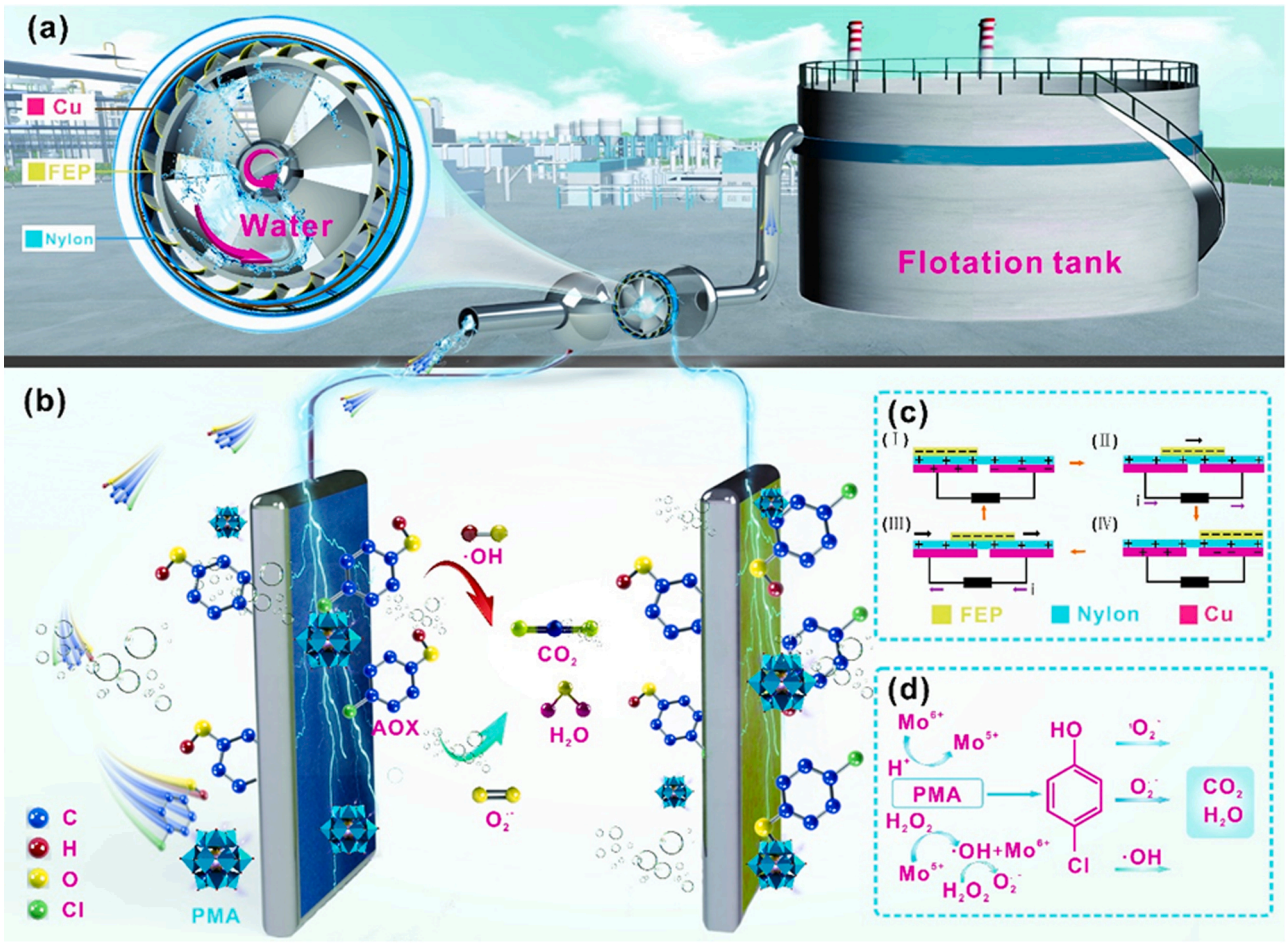

Fig. 1. Self-powered 4-CP degradation system. (a) The mechanical energy of liquid flow is collected and converted into electrical energy by WD-TENG in the pipeline. (b) Schematic diagram of WD-TENG improved 4-CP removal. (c) WD-TENG power generation principle. (d) The scheme of 4-CP degradation.

difficult [26].

Triboelectric nanogenerators (TENGs), an emerging technology for converting mechanical movement into electrical power, have been adopted for self-powered systems in recent years owing to their low cost, flexible design, and excellent adaptability [27–31]. Electrical power, transferred from mechanical movement of TENGs, cooperates with electrochemical techniques to constitute a self-powered electrocatalytic system, which has been applied in wastewater treatment, microbial disinfection, and air pollutant treatment [32–35]. Ye Chen demonstrated self-powered electro-Fenton degradation system, powered by TENGs, for the first time [36]. Since then, many studies have reported that TENGs have great potential as part of self-powered electrochemical systems for environmental treatment by collecting energy from various frequencies of irregular mechanical energy [37–43]. A stable high voltage and the generation of a powerful electric field is the output of a self-powered electrochemical system [44,45]. The powerful electric field cleaves the chemical bonds to remove organic pollutants, such as basic orange 2, methylene blue, and 4-dimethylaminoazobenzene [26, 29,46].

Polyoxometalates are a typical inorganic cluster with various structures, solubilities, and redox potentials and high acidity. This facilitates strong electrochemical processes with multistep redox reactions and multiple electron transfers. POMs' thermal and oxidative stability is their most attractive property, making them suitable as a catalyst for organic synthesis and environmental remediation [47]. Among the various POMs, Keggin-type heteropoly acids (e.g., $H_3PMo_{12}O_{40}$ and $H_3PW_{12}O_{40}$) can catalyze H_2O_2 to generate·OH [18,48].

In this study, a water-driven triboelectric nanogenerator (WD-TENG) with DC output was used to build a self-powered electrochemical system to enhance the 4-CP removal efficiency. The appropriate structure of the WD-TENG and its output performance were investigated. The efficiency of the electrochemical 4-CP treatment process was systematically studied using a powered phosphomolybdic acid/H_2O_2 (PMA/H_2O_2) system. The output of the WD-TENG could reach a voltage of 22 V with a current of 10 μA. The removal of 4-CP improved by 10% in 120 min in the WD-TENG powered electro-PMA/H_2O_2 system. Cooperating with the WD-TENG,·OH played an important role in 4-CP removal, and the spin number was improved from 4.2×10^{15} to 5.0×10^{15}. 4-CP was removed via dichlorination and mineralization by the free radicals. This study provides a promising methodology for improving the performance of self-powered electrochemical processes for the treatment of environmental pollution.

2. Experimental section

2.1. Materials

4-CP (≥99%) was purchased from Sigma-Aldrich·H_2O_2 (30%), while 2,2,6,6-tetramethy l-4-piperidinol (TMP), 5,5-dimethyl-1-pyrroline N-oxide (DMPO), ethanol, chromatographic grade acetonitrile, and phosphomolybdic acid (PMA; $H_3PMo_{12}O_{40}$) were purchased from Aladdin Chemistry Co., Ltd. (Shanghai, China). $Na_2HPO_4.12\ H_2O$ and $NaH_2PO_4.2\ H_2O$ were obtained from Tianjin Zhiyuan Reagent Co. Ltd. (Tianjin, China). All the chemicals were used without further purification.

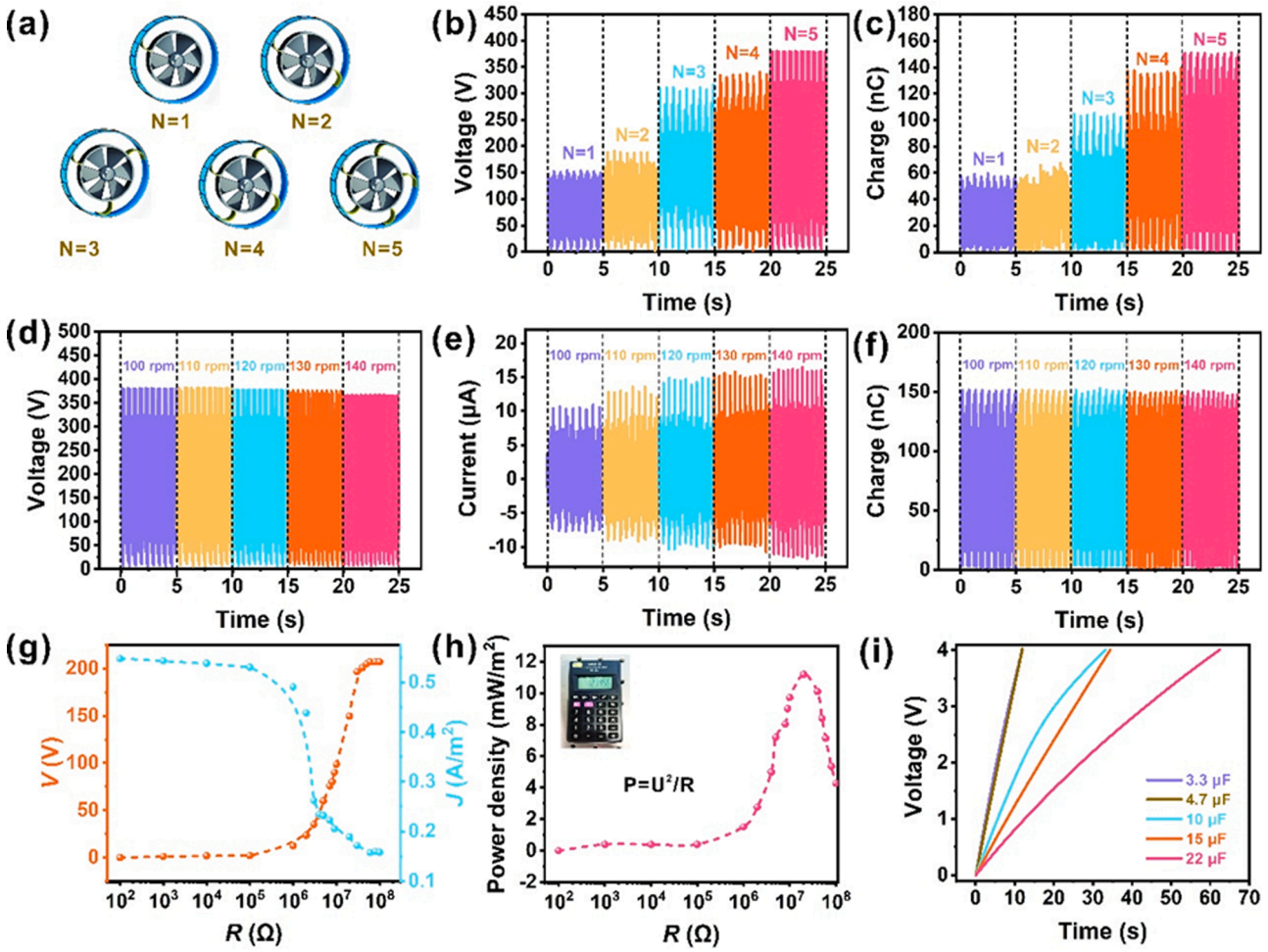

Fig. 2. The performance of WD-TENG. (a) Schematic diagram of WD-TENG with different numbers of FEP films installed. (b) Voltage of WD-TENG with different numbers of FEP films installed. (c) Charge of WD-TENG with different numbers of FEP films installed. (d) Voltage of WD-TENG at different speeds. (e) Current of WD-TENG at different speeds. (f) Charge of WD-TENG at different speeds. (g) The dependence of the output current, voltage on different resistive loads (h) Power density curve. (i) The charging voltage of capacitors with different capacities.

2.2. Fabrication and testing of the WD-TENG

Freestanding triboelectric layer units of the WD-TENG were constructed using a perfluoroethylene propylene (FEP) film, nylon, and Cu foil. The FEP was cut into lengths of 5, 7, and 9 cm with a width of 7 cm and was fixed in the WD-TENG. Nylon was used as the fixed layer and FEP was used as the slide layer of the WD-TENG. Waterproof glue was used to separate the freestanding triboelectric layer units from the water. Different numbers of freestanding triboelectric layer units were installed according to the actual needs. The output performance was measured using an electrometer (Keithley 6514, USA) [49].

2.3. Self-powered electrochemical degradation of 4-CP

The experiments of 4-CP removal were conducted in an oil bath pot, with 0.78 mM 4-CP, 3.9 mM PMA, and 19.5 mM H_2O_2 at 90 °C for 120 min. A buffer consisting of $Na_2HPO_4.12\ H_2O/NaH_2PO_4.2\ H_2O$ (1:3, v/v) was used. Subsequently, 100 mL of the solution was placed in the electrolytic device. The degradation of 4-CP was performed at a rectified current of 10 μA DC supplied by the WD-TENG. Pt was used as the positive electrode, and a glassy carbon electrode was used as the negative electrode.

2.4. Analysis of intermediate products

High-performance liquid chromatography (HPLC, Agilent1100, Agilent Technologies Co Ltd, USA) was used to analyze the concentration of 4-CP. The samples of the residual organic matter were filtered using a 0.22 μm nylon membrane. An Agilent ZORBA XSBC-18 was used as the HPLC column. The mobile phase was a mixture of ultrapure water and acetonitrile at a ratio of 70:30 (v/v) with a flow rate of 1.0 mL/min. Other conditions were as follows: column temperature, 30 °C; injection volume, 10 μL; and analytical wavelength, 280 nm. The intermediate products (4-CC, HQ, and BQ) were also analyzed by gradient elution HPLC with a mobile phase comprising a mixture of ultrapure water and acetonitrile at analytical wavelengths of 289.7, 245.9, and 281.4 nm. The ratio of ultrapure water to acetonitrile was maintained at 80:20 (v/v) for 15 min, and then increased linearly to 10:90 within 15 min

2.5. Determination of free radicals

The free radicals were analyzed using an electron paramagnetic resonance spectrometer (EPR, EMXmicro-6/1/P/L, Karlsruhe, Germany). 5,5-dimethyl-1-pyrroline N-oxide (DMPO) was used as a trapping agent for •OH and superoxide radicals ($•O_2$), whereas 2,2,6,6-tetramethy l-4-piperidinol (TMP) was used for trapping singlet oxygen ($^1O_2$) [50]. Ethanol was used as the scavenger of •OH.

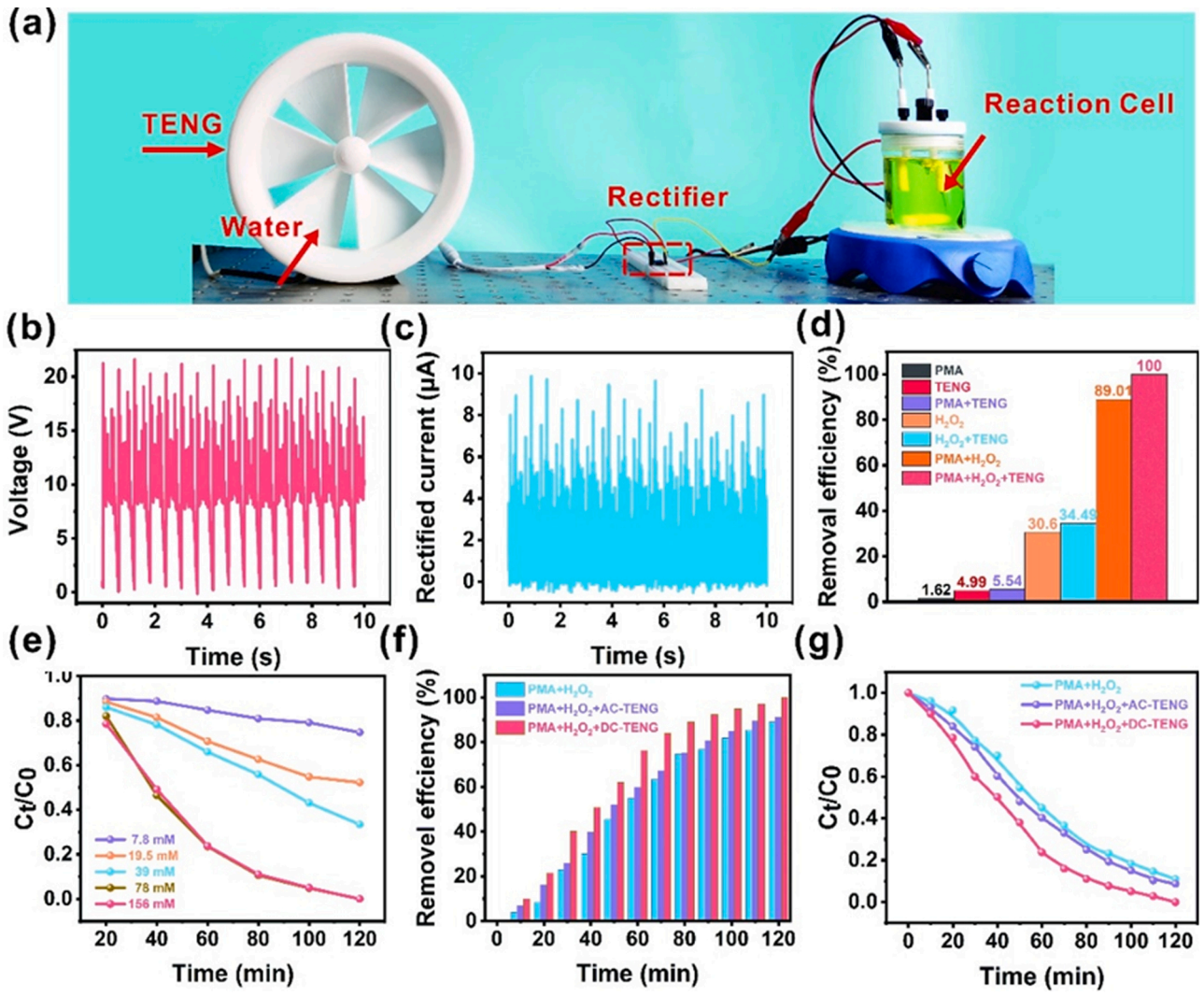

Fig. 3. Self-powered to improve AOX removal efficiency via WD-TENG. (a) Picture of self-powered AOX degradation system. (b) Rectified voltage. (c) Rectified current. (d) The removal efficiency of 4-CP under different reagent. (e) The removal efficiency of 4-CP under different H_2O_2 dosages. (f) The effect before and after rectification on the removal efficiency of 4-CP. (g) The removal performance of 4-CP before and after rectification.

2.6. Analyzation of Mo species in $H_3PMo_{12}O_{40}$

The Mo species were studied using X-ray photoelectron spectroscopy (XPS) on an ESCALAB 250XIþ spectrometer (Thermo Fisher Scientific, USA) with a K Alpha X-ray source. The testing voltage, current, and photoelectron emission angle were 12 kV, 16–25 mA, and 90°, respectively.

3. Results and discussion

3.1. Removing 4-CP by a self-powered electro-PMA/H_2O_2 system

In this study, a water-driven triboelectric nanogenerator (WD-TENG) was designed to collect energy from wastewater flowing in the pipeline, as shown in Fig. 1a. The potential energy generated from the liquid level difference usually gets wasted, because it is too low to drive generators. The WD-TENG was used as a generator in the effluent output pipeline of a flotation tank to capture the mechanical energy of the liquid flow. Electrical energy was supplied to the PMA/H_2O_2 system to remove the 4-CP wastewater (Fig. 1b). Because PMA has excellent redox characteristics, electrical versatility, and high proton conductivity [51], it can catalyze H_2O_2 to mineralize 4-CP using the free radicals [18].

The freestanding triboelectric layer units of the WD-TENG were constructed using a perfluoroethylene propylene (FEP) film, nylon, and Cu foil. The WD-TENG could harvest and convert the potential energy of wastewater into electrical energy. With the wastewater flowing through the turbine, the turbine is turned, which causes relative sliding between the FEP and nylon. Because the electron binding capacities of the materials are different, electrons move from the surface of the nylon to the FEP, leading to an increase in the electric potential on the surface of the Cu foil. This difference in potential causes charge accumulation and current formation, as shown in Fig. 1c. Fig. 1d illustrates the 4-CP degradation scheme. PMA, as an electron medium and proton carrier, can capture electrons and catalyze H_2O_2 to produce more free radicals, such as singlet oxygen, superoxide radicals, and·OH, which can mineralize 4-CP into CO_2 and H_2O.

3.2. Output performance of the WD-TENG

The output performance of the WD-TENG was investigated using different structure angles, lengths of FEP, and numbers of freestanding triboelectric layer units, as shown in Fig. 2. FEP, which contained the -CF_3 group, exhibited the highest charge density [52]. Nylon falls at the positive end of the "triboelectric series," which means it is a best electron donor [53]. Therefore, the contact charge would transfer from nylon, the most positively charged material, to FEP, a negatively

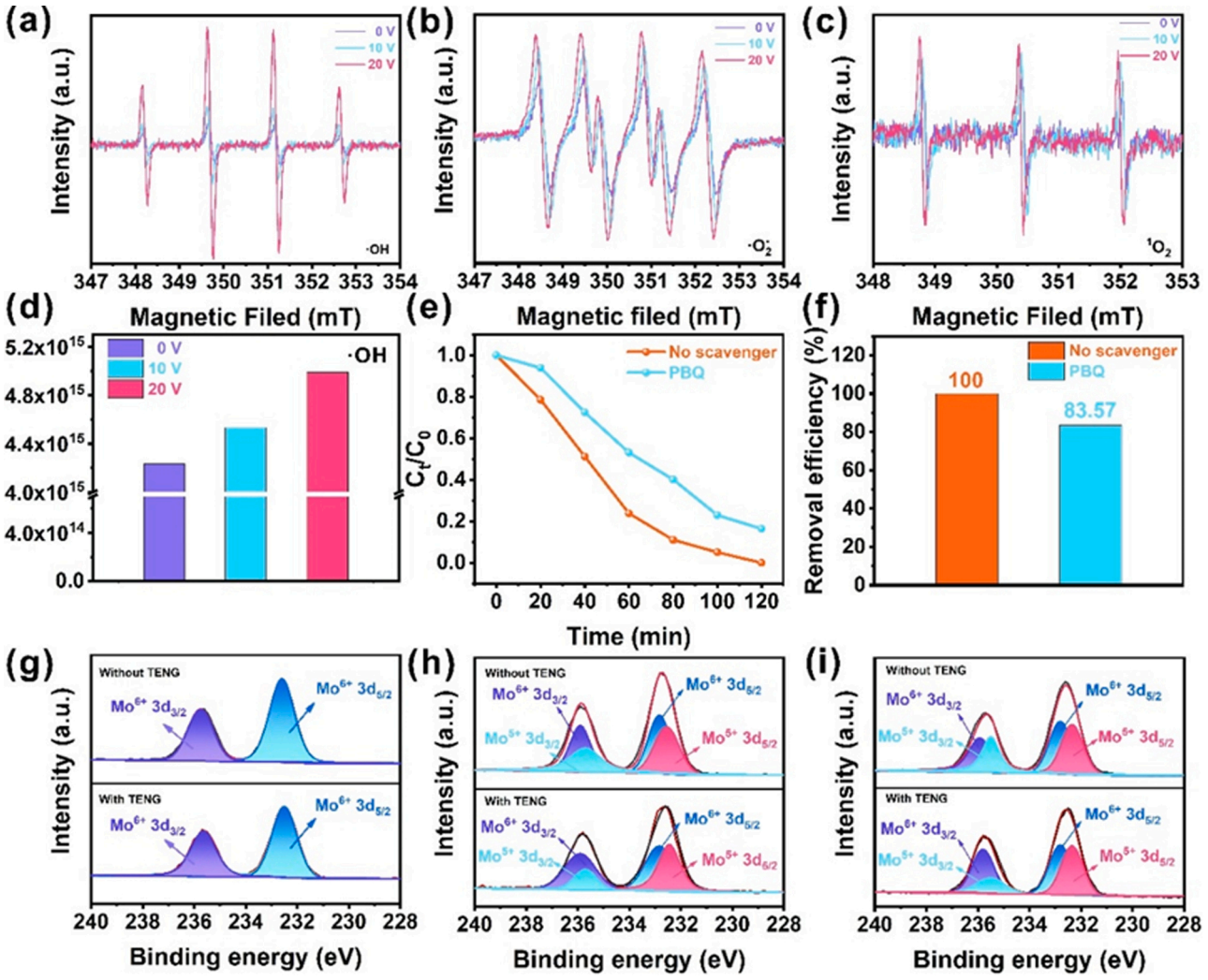

Fig. 4. Self-powered degradation mechanism of AOX. (a) ESR spectra of·OH captured at voltages of 0 V, 10 V, and 20 V. (b) ESR spectra of·O_2^- captured at voltages of 0 V, 10 V, and 20 V. (c) ESR spectra of $^1O_2$ captured at voltages of 0 V, 10 V, and 20 V. (d) Quantitative test of·OH captured at voltages of 0 V, 10 V, and 20 V. (e)·OH capture. (f) Comparison of removal efficiency of·OH capture. (g) Mo species of PMA with and without WD-TENG before the reaction. (h) Mo species of PMA with and without WD-TENG at 30 min (i) Mo species of PMA with and without WD-TENG at 90 min.

charged polymer, during the relative sliding between FEP and nylon. This results in a charge transfer and mechanical energy harvesting from the turbine rotation. The effect of the output performance on the number of freestanding triboelectric layer units is presented in Fig. 2a. The results demonstrate that with increased number of units, both the voltage and electric charge increase. When using five freestanding triboelectric layer units, the voltage and electric charge can reach 380 V and 150 nC, respectively. When the number of units is more than five, the friction of the turbine increases, making it difficult to rotate. Fig. S1 shows the output performance of the WD-TENG with different structural angles (α) between the FEP and turbine. The voltage and current output of the WD-TENG increased with an increase in the angle between the FEP and the turbine, reaching 140 V and 50 nC per unit when $\alpha = 90°$(Figure. S1). A change in α resulted in a change in the friction force, which affected the output of the WD-TENG. As demonstrated in Fig. S2, when the length of the FEP was increased, the voltage and current outputs of the WD-TENG also increased slightly. Thus, five freestanding triboelectric layer units were used with $\alpha = 90°$and FEP $= 9$ cm in the following experiments. Fig. 2d–f exhibits the electrical outputs of the WD-TENG at different rotation speeds. The data show that the open-circuit voltage and short-circuit current values are stable and can be maintained at approximately 380 V and 150 nC, respectively. The short-circuit current increases with the rotation speed, reaching 15 μA at 140 rpm, while the output performance of the WD-TENG has a slight influence on the rotation speed. This could be due to the accumulation of static charge resulting from improved rotation speed, which speeds up the electron flow in the external circuitry, although the contact state does not change between the friction materials. The dependence of the output current and voltage on different resistive loads and power density is presented in Fig. 2 g and 2 f. The output voltage increased with an increase in the resistance, but the change in current showed the opposite trend. Because internal resistance exists in the WD-TENG, a maximum peak power of 11.5 mW/m^2 could be obtained under an external resistance of 100 MΩ. Charging capacitors with different capacities were tested to collect electricity using the WD-TENG, as shown in Fig. 2 h. A capacitor of 4.7 μF could be charged to 4 V within 30 s, confirming that the capacitor can effectively store an electric charge. These results suggest that the WD-TENG can be used as an independent power source for electrochemistry.

3.3. Removal of 4-CP using a self-powered electrochemical process

PMA can catalyze H_2O_2 to generate free radicals by obtaining electrons from 4-CP, resulting in the reduction of PMA(Mo^{6+}) to PMA(Mo^{5+})·H_2O_2 also can oxidize PMA(Mo^{5+}) back to PMA(Mo^{6+}) by releasing free radicals, such as singlet oxygen, superoxide radicals,

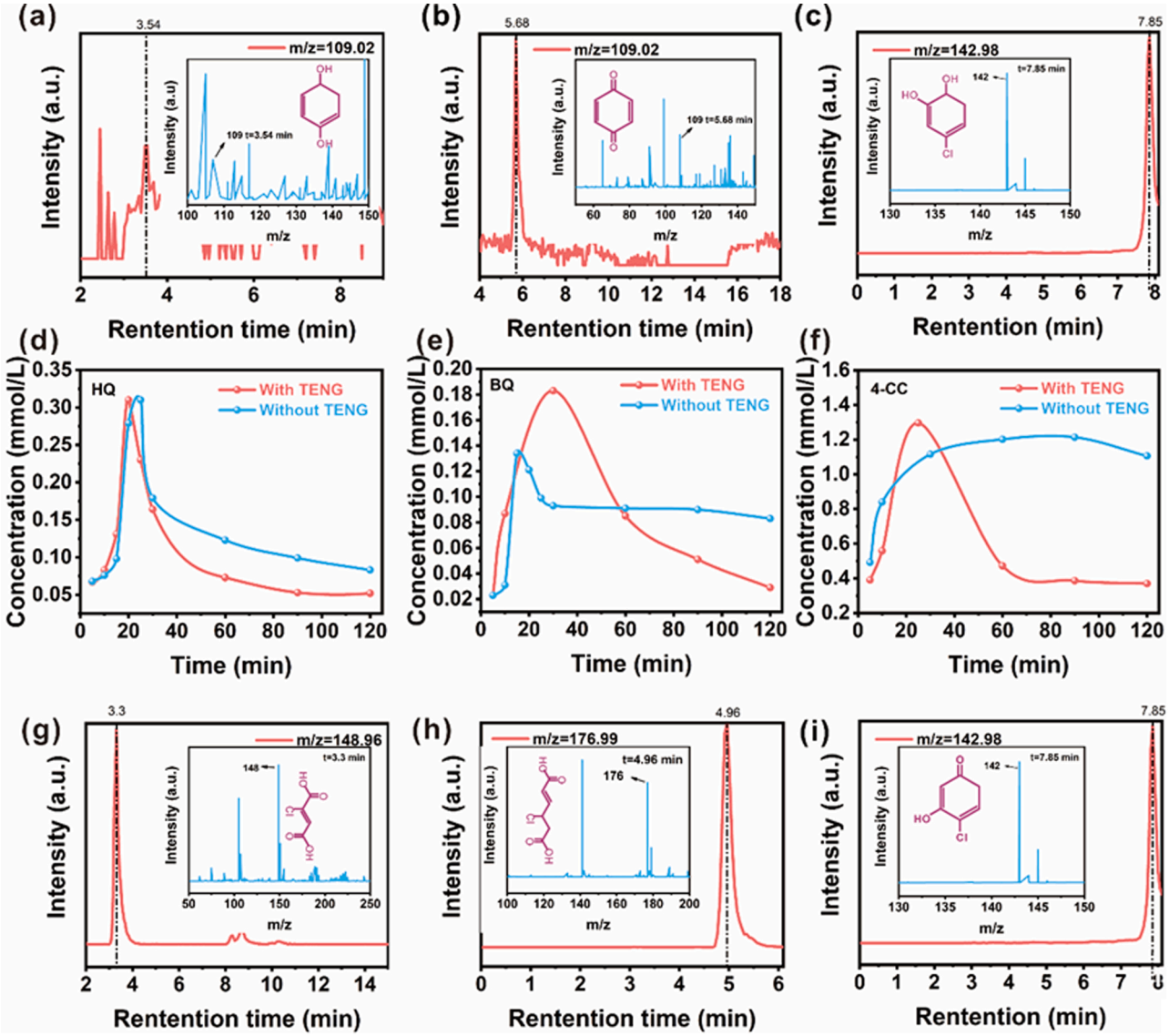

Fig. 5. Intermediate products in self-powered 4-CP removal process. (a) HQ, (b) BQ and (c) 4-CC. (d) Concentration of HQ generated during degradation. (e) Concentration of BQ generated during degradation. (f) Concentration of 4-CC generated during degradation. (g) 2-chlorofumaric acid. (h) (E)– 4-chlorohex-2-enedioic acid. (i) 4-chloro-3-hydroxycyclohexa-2.4-dienone.

and·OH [18]. However, the *p* orbitals of the O atoms mainly contribute to the formation of the highest occupied molecular orbital (HOMO), which means that the electrons of oxygen atoms are easily shared with other atoms. The *d* orbitals of metallic Mo and *p* orbitals of the P atoms predominantly contribute to the formation of the LUMO orbital [54]. Furthermore, Mo and P are intermolecular PMA molecules, which make PMA a good proton conductor but a somewhat poor electron conductor [51]. The poor electron conductivity limits the conversion efficiency of PMA(Mo^{5+}), resulting in poor catalytic properties. The WD-TENG-enhanced PMA/H_2O_2 system was constructed for 4-CP removal, as shown in Fig. 3a. Electrons could be captured by PMA (Mo^{6+}), and H_2O_2 could obtain electrons to generate·OH in an electric field [55]. A stable voltage and current were output by the WD-TENG. As demonstrated in Figs. 3b and 3c, the rectified voltage and current were approximately 22 V and 10 μA, respectively. Although a high-voltage output could be implied, the removal rate of 4-CP only increased from 30.6% (without WD-TENG) to 34.49%. This could be due to the poor current output, which could not provide sufficient electrons to H_2O_2 to oxidize 4-CP. PMA significantly improved the removal rate of 4-CP by H_2O_2, which reached 89.01% after 120 min. With the effect of the electric field and electrons supplied by the WD-TENG, PMA and H_2O_2 were both activated, leading to the removal of 4-CP reaching 100% (Fig. 3d)·H_2O_2 also played a key role in the removal of 4-CP. When the concentration of H_2O_2 was less than 39 Mmol/L, there were insufficient free radicals to attack the 4-CP, leading to a 4-CP removal rate of approximately 40% after 120 min (Fig. 3e); while, when the concentration of H_2O_2 was high enough to supply sufficient hydroxyl groups to the system, 4-CP could be transformed to unstable intermediates and then mineralized further, as shown in Figs. 3f and 3g. However, while the alternating current (AC) was rectified to direct current (DC), the energy would be saved by avoiding the eddy current loss of AC. The 4-CP removal efficiency was improved, and the lower concentration of 4-CP can be obtained (Figs. 3f and 3g).

3.4. Degradation mechanism of 4-CP

The standard reduction potential (E°) of H_2O_2 is 1.76 V/SHE [56]. However, H_2O_2 initiates the formation of the radicals at the given potential, such as·OH with higher oxidation power (E° = 2.80 V/SHE), hydroperoxyl radicals ($HO_2^\bullet$) (E° = 1.65 V/SHE), superoxide anion

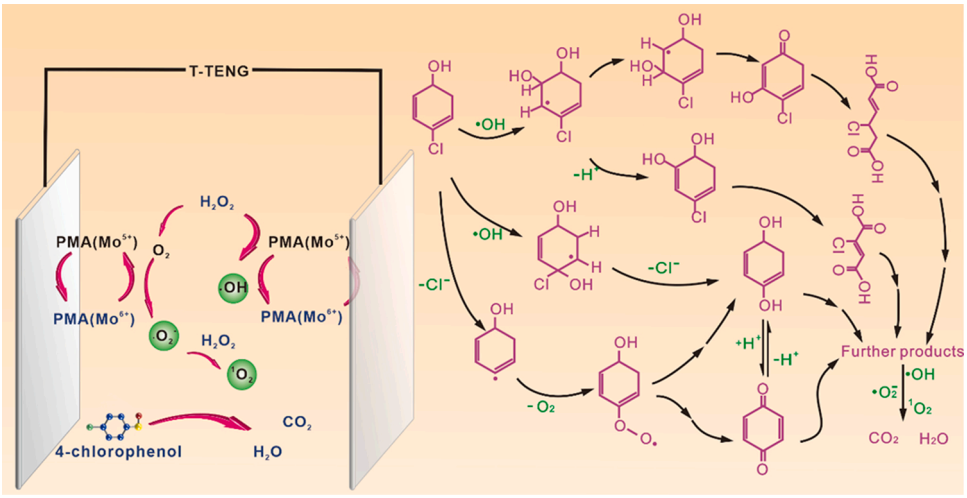

Fig. 6. the possible scheme of 4-CP degradation in self-powered 4-CP removal process.

radicals ($^{\bullet}O_2^-$), and singlet oxygen ($^1O_2$) [57,58]. These free radicals were detected at 0 V, 10 V, and 20 V using the electron spin resonance. Fig. 4a depicts the 4-fold peaks with an intensity ratio of 1:2:2:1, indicating the generation of·OH [59]. The signals of $^{\bullet}O_2^-$ and $^1O_2$ were enhanced by increasing the voltage, as shown in Figs. 4b and 4c. Owing to the electric field from the WD-TENG, the spin number of·OH increased by 25%, from 4.2×10^{15} to 5.0×10^{15} (Fig. 4d). The spin number of $^{\bullet}O_2^-$ is approximate to 1.5×10^{15} at 20 V (Fig. S4). However, the spin number of $^1O_2$ increased from 6×10^{12} to 8.6×10^{13}. This would be due to the generating of $^1O_2$ converted from·O_2^- and·OH-mediated pathways through the Haber-Weiss reaction [57].

To confirm the effect of·OH, PBQ was used to capture·OH, as demonstrated in Figs. 4e and 4 f. The removal rate decreased 17.43%. Though without the effect of·OH, the removal rate of 4-CP still can reach to 83.57%, indicating that·O_2 − and $^1O_2$ also affected the 4-CP removal. In PMA/H_2O_2 system, PMA (Mo^{6+}) obtains electrons to form PMA (Mo^{5+}) by obtaining electrons from H_2O_2 or 4-CP (Eq. 1) [18]. PMA (Mo^{5+}) performed good catalytic activities to efficiently active H_2O_2 with releasing·OH (Eq. 2) [60].

$$4\text{-CP} + \text{PMA}(Mo^{6+}) + H^+ \rightarrow \text{oxidized products} + \text{PMA}(Mo^{5+}) \quad (1)$$

$$\text{PMA}(Mo^{5+}) + H_2O_2 \rightarrow \text{PMA}(Mo^{6+}) + OH^- + \bullet OH \quad (2)$$

The XPS spectra of PMA reacting with H_2O_2 indicates that the conversion efficiency of PMA(Mo^{5+}) was sped up owing to the effect of T-TNEG (Fig. 4g-i and Fig. S3). The high conversion efficiency between PMA(Mo^{5+}) and PMA(Mo^{6+}) could generate more·OH from H_2O_2.

The series of oxidation intermediate products of 4-CP were analyzed (Fig. 5). 4-chlorocatechol (4-CC), hydroquinone (HQ), and benzoquinone (BQ) were found in the WD-TENG-powered electro-PMA/H_2O_2 system, because these are the primary oxidation products of 4-CP [61]. With the effect of the electric field and electrons supplied by the WD-TENG, PMA and H_2O_2 were both activated, and the generation of·OHs was promoted. The increased·OHs attacks HQ and converts it to HHQ or BQ. Fig. 5d demonstrates that the concentration decreased sharply after 20 min, indicating that HQ could be attacked by free radicals, even though it is more stable than 4-CP. With the effect of the WD-TENG, the concentration of BQ was higher, reaching 1.8 mmol/L at 40 min, compared to that without the WD-TENG, which implies that some BQ was converted from the HQ. 4-CC, the second main intermediate product, seemed to degrade more easily under the effect of the WD-TENG, as shown in Fig. 5f. These intermediate products were further oxidized. Additional intermediate molecules were identified, such as 2-chlorofumaric acid, (E)− 4-chlorohex-2-enedioic acid, and 4-chloro-3-hydroxycyclohexa-2.4-dienone.

Based on the above results, the possible pathways of 4-CP are illustrated in Fig. 6. 4-CP is converted to 4-CC, HQ, or BQ via dichlorination or oxidation.·OH is added at the ortho position of the hydroxyl group of 4-CP. The aromatic ring is then recovered by the elimination of a hydrogen atom, which forms 4-CC. When·OH attacks the para position or chlorine atom of 4-CP, or an electron occupies the para position of the generated intermediate, it leads to the release of a chloride ion. HQ can either be oxidized to BQ [62] or can be converted to hydroxyhydroquinone (HHQ) owing to the·OH attack, but HHQ is unstable and is further oxidized to hydroxybenzoquinone (HBQ) or other products. 4-CC can be degraded into small molecular fragments by a ring-opening reaction. These intermediate products may be further mineralized into CO_2 and H_2O by the free radicals.

4. Conclusions

In summary, this work demonstrates a self-powered wastewater treatment system that is efficient in enhancing and powering WD-TENG. The WD-TENG was constructed with an appropriate multiple-structure, low cost, and high efficiency. It provided a high voltage and stable current output for the electro-PMA/H_2O_2 system with a rectified voltage and rectified current of approximately 22 V and 10 μA, respectively. Cooperating with the WD-TENG,·OH played a key role in 4-CP removal, and the spin number was improved from 4.2×10^{15} to 5.0×10^{15}, resulting in a 10% improvement in the removal of 4-CP. 4-CP is removed predominantly by dichlorination and mineralization by free radicals. The mechanism of the self-powered electro-PMA/H_2O_2 system and possible pathways of 4-CP degradation were systematically explained based on the experiments. This study provides a promising methodology for improving the performance of self-powered electrochemical processes for treating environmental pollution.

CRediT authorship contribution statement

Xinliang Liu and Shuangxi Nie conceived the idea and designed the experiment. Jilong Mo and Wanhai Wu carried out the materials characterization and fabricated the devices. Wanhai Wu and Hainong Song performed the electrical measurement. Jilong Mo, Xinliang Liu and Shuangxi Nie wrote the manuscript. All the authors discussed the results and commented on the manuscript.

Declaration of Competing Interest

The authors declare that they have no known competing financial interests or personal relationships that could have appeared to influence

the work reported in this paper.

Acknowledgments

This research was supported by the National Natural Science Foundation of China (grant number 31971604), the Natural Science Foundation of Guangxi Province (grant number 2018GXNSFDA281050), and the Opening Project of National Enterprise Technology Center of Guangxi Bossco Environmental Protection Technology Co., Ltd, Nanning 530007, China (grant number GXU-BFY-2020-029).

Appendix A. Supporting information

Supplementary data associated with this article can be found in the online version at doi:10.1016/j.apcatb.2022.121422.

References

[1] S. Nie, K. Zhang, X. Lin, D. Yan, H. Liang, S. Wang, Enzymatic pretreatment for the improvements of dispersion and film properties of cellulose nanofibrils, Carbohydr. Polym. 181 (2018) 1136–1142.
[2] S. Nie, X. Liu, Z. Wu, L. Zhan, G. Yin, S. Yao, H. Song, S. Wang, Kinetics study of oxidation of the lignin model compounds by chlorine dioxide, Chem. Eng. J. 241 (2014) 410–417.
[3] S. Nie, S. Wang, C. Qin, S. Yao, J.F. Ebonka, X. Song, K. Li, Removal of hexenuronic acid by xylanase to reduce adsorbable organic halides formation in chlorine dioxide bleaching of bagasse pulp, Bioresour. Technol. 196 (2015) 413–417.
[4] F. Dong, Z. Pang, S. Yang, Q. Lin, S. Song, C. Li, X. Ma, S. Nie, Improving Wastewater Treatment by Triboelectric-Photo/Electric Coupling Effect, ACS Nano.16 (2022) 3449–3475.
[5] J.-C. Hong, M.-Y. Hwang, C.-M. Tsai, M.-C. Liu, Y.-F. Lee, Exploring teachers' attitudes toward implementing new ICT educational policies, Interact. Learn. Environ. (2020) 1–15.
[6] S. Xie, M. Li, Y. Liao, Q. Qin, S. Sun, Y. Tan, In-situ preparation of biochar-loaded particle electrode and its application in the electrochemical degradation of 4-chlorophenol in wastewater, Chemosphere 273 (2021).
[7] S. Anandhakumar, M. Chandrasekaran, M. Noel, Anodic oxidation of chlorophenols in micelles and microemulsions on glassy carbon electrode: the medium effect on electroanalysis and electrochemical detoxification, J. Appl. Electrochem. 40 (2010) 303–310.
[8] M. Zhang, L. Zhi, H. Li, H. Long, W. Zhao, Process integration of halogenation and oxidation for recovery and removal of phenols from high strength phenolic wastewater, Chem. Eng. J. 229 (2013) 99–104.
[9] O. Hamdaoui, E. Naffrechoux, Sonochemical and photosonochemical degradation of 4-chlorophenol in aqueous media, Ultrason. Sonochem. 15 (2008) 981–987.
[10] S. Mubarik, A. Saeed, M.M. Athar, M. Iqbal, Characterization and mechanism of the adsorptive removal of 2,4,6-trichlorophenol by biochar prepared from sugarcane baggase, J. Ind. Eng. Chem. 33 (2016) 115–121.
[11] J. Matos, A. Garcia, T. Cordero, J.M. Chovelon, C. Ferronato, Eco-friendly TiO2-AC photocatalyst for the selective photooxidation of 4-chlorophenol, Catal. Lett. 130 (2009) 568–574.
[12] S.E. Sanni, O. Philemon, E.E. Okoro, B.A. Oni, T.A. Idowu, O. Adegbite, Heterogeneous catalytic conversion of 4-chlorophenol via atomic hydrogen substitution induced by size-controlled polydisperse nanocobalt, Chem. Eng. Sci. 247 (2022), 117018.
[13] J. Zhao, Y. Li, Y. Li, H. Yang, D. Hu, H. Zhang, Effects of 4-chlorophenol toxicity on sludge performance and microbial community in sequencing batch reactors, J. Environ. Sci. Health, Part A 54 (2019) 508–515.
[14] S. Xie, M. Li, Y. Liao, Q. Qin, S. Sun, Y. Tan, In-situ preparation of biochar-loaded particle electrode and its application in the electrochemical degradation of 4-chlorophenol in wastewater, Chemosphere 273 (2021), 128506.
[15] N.A. Bury, K.A. Mumford, G.W. Stevens, The electro-Fenton regeneration of Granular Activated Carbons: degradation of organic contaminants and the relationship to the carbon surface, J. Hazard. Mater. 416 (2021), 125792.
[16] A.D. Bokare, W. Choi, Review of iron-free Fenton-like systems for activating H2O2 in advanced oxidation processes, J. Hazard. Mater. 275 (2014) 121–135.
[17] Y. Wang, G. Zhang, Y. Xue, J. Tang, X. Shi, C. Zhang, In situ anodic induction of low-valence copper in electro-Fenton system for effective nitrobenzene degradation, Environ. Sci. Pollut. Res. 26 (2019) 32165–32174.
[18] M. Lei, Q. Gao, K.M. Zhou, P. Gogoi, J. Liu, J.B. Wang, H.N. Song, S.F. Wang, X. L. Liu, Catalytic degradation and mineralization mechanism of 4-chlorophenol oxidized by phosphomolybdic acid/H2O2, Sep. Purif. Technol. 257 (2021) 8.
[19] E. Brillas, I. Sirés, M.A. Oturan, Electro-Fenton process and related electrochemical technologies based on Fenton's reaction chemistry, Chem. Rev. 109 (2009) 6570–6631.
[20] J.J. Pignatello, E. Oliveros, A. MacKay, Advanced oxidation processes for organic contaminant destruction based on the Fenton reaction and related chemistry, Crit. Rev. Environ. Sci. Technol. 36 (2006) 1–84.
[21] X. Hou, X. Huang, Z. Ai, J. Zhao, L. Zhang, Ascorbic acid/Fe@Fe2O3: a highly efficient combined Fenton reagent to remove organic contaminants, J. Hazard. Mater. 310 (2016) 170–178.
[22] P.V. Nidheesh, R. Gandhimathi, Trends in electro-Fenton process for water and wastewater treatment: an overview, Desalination 299 (2012) 1–15.
[23] L. Rizzo, Bioassays as a tool for evaluating advanced oxidation processes in water and wastewater treatment, Water Res. 45 (2011) 4311–4340.
[24] Y. Zhu, C. Chen, M. Tian, Y. Chen, Y. Yang, S. Gao, Self-powered electro-Fenton degradation system using oxygen-containing functional groups-rich biomass-derived carbon catalyst driven by 3D printed flexible triboelectric nanogenerator, Nano Energy 83 (2021), 105720.
[25] X. Qin, K. Zhao, X. Quan, P. Cao, S. Chen, H. Yu, Highly efficient metal-free electro-Fenton degradation of organic contaminants on a bifunctional catalyst, J. Hazard. Mater. 416 (2021).
[26] Y. Chen, Y. Zhu, M. Tian, C. Chen, X. Jia, S. Gao, Sustainable self-powered electro-Fenton degradation of organic pollutants in wastewater using carbon catalyst with controllable pore activated by EDTA-2Na, Nano Energy 59 (2019) 346–353.
[27] K. Han, J. Luo, Y. Feng, L. Xu, W. Tang, Z.L. Wang, Self-powered electrocatalytic ammonia synthesis directly from air as driven by dual triboelectric nanogenerators, Energy Environ. Sci. 13 (2020) 2450–2458.
[28] C. Wu, A.C. Wang, W. Ding, H. Guo, Z.L. Wang, Triboelectric nanogenerator: a foundation of the energy for the new era, Adv. Energy Mater. 9 (2019), 1802906.
[29] C. Ning, R. Cheng, Y. Jiang, F. Sheng, J. Yi, S. Shen, Y. Zhang, X. Peng, K. Dong, Z. L. Wang, Helical fiber strain sensors based on triboelectric nanogenerators for self-powered human respiratory monitoring, ACS Nano (2022).
[30] A. Wei, X. Xie, Z. Wen, H. Zheng, H. Lan, H. Shao, X. Sun, J. Zhong, S.-T. Lee, Triboelectric nanogenerator driven self-powered photoelectrochemical water splitting based on hematite photoanodes, ACS Nano 12 (2018) 8625–8632.
[31] Y. Liu, J. Mo, Q. Fu, Y. Lu, N. Zhang, S. Wang, S. Nie, Enhancement of triboelectric charge density by chemical functionalization, Adv. Funct. Mater. 30 (2020) 2004714.
[32] L. Zhou, L. Liu, W. Qiao, Y. Gao, Z. Zhao, D. Liu, Z. Bian, J. Wang, Z.L. Wang, Improving degradation efficiency of organic pollutants through a self-powered alternating current electrocoagulation system, ACS Nano 15 (2021) 19684–19691.
[33] S. Shen, J. Fu, J. Yi, L. Ma, F. Sheng, C. Li, T. Wang, C. Ning, H. Wang, K. Dong, Z. L. Wang, High-efficiency wastewater purification system based on coupled photoelectric–catalytic action provided by triboelectric nanogenerator, Nano Micro Lett. 13 (2021) 194.
[34] N. Zhai, Z. Wen, X. Chen, A. Wei, M. Sha, J. Fu, Y. Liu, J. Zhong, X. Sun, Blue energy collection toward all-hours self-powered chemical energy conversion, Adv. Energy Mater. 10 (2020), 2001041.
[35] S. Nie, Q. Fu, X. Lin, C. Zhang, Y. Lu, S. Wang, Enhanced performance of a cellulose nanofibrils-based triboelectric nanogenerator by tuning the surface polarizability and hydrophobicity, Chem. Eng. J. 404 (2021) 126512.
[36] Y. Chen, M. Wang, M. Tian, Y. Zhu, X. Wei, T. Jiang, S. Gao, An innovative electro-fenton degradation system self-powered by triboelectric nanogenerator using biomass-derived carbon materials as cathode catalyst, Nano Energy 42 (2017) 314–321.
[37] Y. Zhu, M. Tian, Y. Chen, Y. Yang, X. Liu, S. Gao, 3D printed triboelectric nanogenerator self-powered electro-Fenton degradation of orange IV and crystal violet system using N-doped biomass carbon catalyst with tunable catalytic activity, Nano Energy 83 (2021).
[38] S. Gao, M. Wang, Y. Chen, M. Tian, Y. Zhu, X. Wei, T. Jiang, An advanced electro-Fenton degradation system with triboelectric nanogenerator as electric supply and biomass-derived carbon materials as cathode catalyst, Nano Energy 45 (2018) 21–27.
[39] Y. Feng, K. Han, T. Jiang, Z. Bian, X. Liang, X. Cao, H. Li, Z.L. Wang, Self-powered electrochemical system by combining Fenton reaction and active chlorine generation for organic contaminant treatment, Nano Res. 12 (2019) 2729–2735.
[40] Y. Feng, L. Zhang, Y. Zheng, D. Wang, F. Zhou, W. Liu, Leaves based triboelectric nanogenerator (TENG) and TENG tree for wind energy harvesting, Nano Energy 55 (2019) 260–268.
[41] C. Chen, Y. Zhu, M. Tian, Y. Chen, Y. Yang, K. Jiang, S. Gao, paper Sustainable self-powered electro-Fenton degradation using N, S co-doped porous carbon catalyst fabricated with adsorption-pyrolysis-doping strategy, Nano Energy 81 (2021).
[42] J. Mo, Y. Liu, Q. Fu, C. Cai, Y. Lu, W. Wu, Z. Zhao, H. Song, S. Wang, S. Nie, Triboelectric nanogenerators for enhanced degradation of antibiotics via external electric field, Nano Energy 93 (2022), 106842.
[43] S. Li, J. Jiang, N. Zhai, J. Liu, K. Feng, Y. Chen, Z. Wen, X. Sun, J. Zhong, A half-wave rectifying triboelectric nanogenerator for self-powered water splitting towards hydrogen production, Nano Energy 93 (2022), 106870.
[44] C. Cai, B. Luo, Y. Liu, Q. Fu, T. Liu, S. Wang, S. Nie, Advanced triboelectric materials for liquid energy harvesting and emerging application, Mater. Today 52 (2022) 299–326.
[45] C. Zhang, X. Lin, N. Zhang, Y. Lu, Z. Wu, G. Liu, S. Nie, Chemically functionalized cellulose nanofibrils-based gear-like triboelectric nanogenerator for energy harvesting and sensing, Nano Energy 66 (2019), 104126.
[46] X. Wei, Z. Wen, Y. Liu, N. Zhai, A. Wei, K. Feng, G. Yuan, J. Zhong, Y. Qiang, X. Sun, Hybridized mechanical and solar energy-driven self-powered hydrogen production, Nano-Micro Lett. 12 (2020) 88.
[47] A. Proust, B. Matt, R. Villanneau, G. Guillemot, P. Gouzerh, G. Izzet, Functionalization and post-functionalization: a step towards polyoxometalate-based materials, Chem. Soc. Rev. 41 (2012) 7605–7622.
[48] M. Taghavi, M. Tabatabaee, M.H. Ehrampoush, M.T. Ghaneian, M. Afsharnia, A. Alami, J. Mardaneh, Synthesis, characterization and photocatalytic activity of TiO2/ZnO-supported phosphomolybdic acid nanocomposites, J. Mol. Liq. 249 (2018) 546–553.

[49] Y. Liu, Q. Fu, J. Mo, Y. Lu, C. Cai, B. Luo, S. Nie, Chemically tailored molecular surface modification of cellulose nanofibrils for manipulating the charge density of triboelectric nanogenerators, Nano Energy 89 (2021) 106369.
[50] M. Wei, X. Shi, L. Xiao, H. Zhang, Synthesis of polyimide-modified carbon nanotubes as catalyst for organic pollutant degradation via production of singlet oxygen with peroxymonosulfate without light irradiation, J. Hazard. Mater. 382 (2020), 120993.
[51] W. Chen, X. Wei, Y. Zhang, Phosphomolybdic acid modified PtRu nanocatalysts for methanol electro-oxidation, J. Appl. Electrochem. 43 (2013) 575–582.
[52] S. Li, J. Nie, Y. Shi, X. Tao, F. Wang, J. Tian, S. Lin, X. Chen, Z.L. Wang, Contributions of different functional groups to contact electrification of polymers, Adv. Mater. 32 (2020), 2001307.
[53] A.F. Diaz, R.M. Felix-Navarro, A semi-quantitative tribo-electric series for polymeric materials: the influence of chemical structure and properties, J. Electrost. 62 (2004) 277–290.
[54] C. Zhou, C. Wang, G. Fan, L. Deng, DFT study on capacitive property of composites built by phosphomolybdic acid with nitrogen-doped graphene, J. Inorg. Organomet. Polym. Mater. 31 (2021) 4473–4479.
[55] J. Wang, S. Li, Q. Qin, C. Peng, Sustainable and feasible reagent-free electro-Fenton via sequential dual-cathode electrocatalysis, Proc. Natl. Acad. Sci. 118 (2021), e2108573118.
[56] K.M. Nair, V. Kumaravel, S.C. Pillai, Carbonaceous cathode materials for electro-Fenton technology: mechanism, kinetics, recent advances, opportunities and challenges, Chemosphere 269 (2021), 129325.
[57] Y. Zhu, F. Deng, S. Qiu, F. Ma, Y. Zheng, L. Gao, A self-sufficient electro-Fenton system with enhanced oxygen transfer for decontamination of pharmaceutical wastewater, Chem. Eng. J. 429 (2022), 132176.
[58] B. Jain, A.K. Singh, H. Kim, E. Lichtfouse, V.K. Sharma, Treatment of organic pollutants by homogeneous and heterogeneous Fenton reaction processes, Environ. Chem. Lett. 16 (2018) 947–967.
[59] Q. Fu, Y. Liu, J. Mo, Y. Lu, C. Cai, Z. Zhao, S. Wang, S. Nie, Improved capture and removal efficiency of gaseous acetaldehyde by a self-powered photocatalytic system with an external electric field, ACS Nano 15 (2021) 10577–10586.
[60] X. Chen, J. Wang, Y. Yu, H. Chen, X. Wu, S. Gao, The fabrication of PMo11Fe cluster supporting on SBA-15 and catalytic epoxidation of cyclooctene with H2O2 as oxidant, Catal. Lett. (2022).
[61] Z. Han, D. Zhang, Y. Sun, C. Liu, Reexamination of the reaction of 4-chlorophenol with hydroxyl radical, Chem. Phys. Lett. 474 (2009) 62–66.
[62] J. Theurich, M. Lindner, D.W. Bahnemann, Photocatalytic degradation of 4-chlorophenol in aerated aqueous titanium dioxide suspensions: a kinetic and mechanistic study, Langmuir 12 (1996) 6368–6376.